



HAL
open science

Treatment of household product emissions in indoor air: Real scale assessment of the removal processes

P. Harb, N. Locoge, F. Thevenet

► To cite this version:

P. Harb, N. Locoge, F. Thevenet. Treatment of household product emissions in indoor air: Real scale assessment of the removal processes. *Chemical Engineering Journal*, 2020, 380, pp.122525. 10.1016/j.cej.2019.122525 . hal-02913605

HAL Id: hal-02913605

<https://hal.science/hal-02913605>

Submitted on 20 Jul 2022

HAL is a multi-disciplinary open access archive for the deposit and dissemination of scientific research documents, whether they are published or not. The documents may come from teaching and research institutions in France or abroad, or from public or private research centers.

L'archive ouverte pluridisciplinaire **HAL**, est destinée au dépôt et à la diffusion de documents scientifiques de niveau recherche, publiés ou non, émanant des établissements d'enseignement et de recherche français ou étrangers, des laboratoires publics ou privés.



Distributed under a Creative Commons Attribution - NonCommercial 4.0 International License

Treatment of household product emissions in indoor air: real scale assessment of the removal processes.

P. Harb, N. Locoge and F. Thevenet*

IMT Lille Douai, Université de Lille, SAGE, F-59000 Lille, France

Abstract

Domestic activities involving household products are transient but intense indoor sources of VOCs. Once emitted, pollutants can be processed by indoor air treatment devices. To provide operational conclusions on VOC emissions and their removal by treatment systems, this study explores the issue at real scale: (i) operation of a 40 m³ experimental room, (ii) representative housecleaning action, and (iii) implementation of selected and commercially available treatment devices. The objective is to challenge the current standards by exploring the behavior of representative air treatment systems and providing a comprehensive characterization of their performances and impacts. First, VOC emissions of selected housecleaning product are characterized as a function of temperature and RH (relative humidity) in the experimental room *IRINA*. Limonene is identified as a tracer of household product emissions, its removal is investigated. This approach allows discriminating the device performances and identifying the contributions of sorption, photolysis, ozonolysis and photocatalysis in the removal processes. Depending on the media, sorptive and

photocatalytic removal are highly contrasted. Third, gas phase side-products generated by each air treatment device are addressed at start up and after 8 hours of operation. Remarkably, secondary organic aerosols are identified as side-products of limonene photocatalytic processing. Finally, respective contributions of treated limonene, gas phase and particulate side-products are evaluated through the carbon mass balance of the treatment processes. While the current standard evaluations report equivalent performances for both devices, their real scale evaluation evidence contrasted behaviors. This study shows the effectiveness of providing a comprehensive and real scale characterization of the performances of air treatment devices. It evidences the prospect of moving current experimental approaches related to indoor air investigations to realistic scale and conditions.

***Corresponding author:** F. Thevenet; email address: frederic.thevenet@imt-lille-douai.fr

Keywords: air treatment, household products, VOC emissions, photocatalysis, limonene

1. Introduction

Domestic activities such as household actions are transient but intense and specific indoor sources of volatile organic compounds (VOCs) [1]. Thereby, the use of cleaning products induces recurrent exposures of occupants to high concentrations of VOCs and impacts indoor air quality. Among other terpenes, limonene is widely employed in air fresheners and household cleaners for its odorous property [1-4]. Recent field campaigns evidenced that d-limonene is an ubiquitous indoor air pollutant in various indoor environments such as homes [5], offices [6] and schools [7]. In spite of the fact that monitored d-limonene concentrations during abovementioned campaigns do not exceed $19 \mu\text{g m}^{-3}$ [7], such terpene emissions in indoor environments from household products may lead to secondary organic aerosol (SOA) formation and carbonyl VOC production in the presence of ozone as evidenced by Rossignol et al. [8]. Among the 51 cleaning products investigated and characterized in the ADOQ project [9], the housecleaning product labeled ADOQ-50 contains up to 2 %wt. of d-limonene in its liquid form. The use of ADOQ-50 in the experimental house MARIA confirmed high emission rates of limonene, leading to transient but intense indoor concentrations of limonene ranging from 149 to $400 \mu\text{g m}^{-3}$ during summer and winter campaigns respectively [9].

Limonene is a widely studied and highly reactive terpenoid, however, while its ozonolysis is largely investigated for atmospheric chemistry purposes [1-4, 8-16], limonene reactivity in indoor environments is far less studied [17-19]. Limonene indoor reactivity has been scarcely addressed through photocatalytic oxidation processes, but with ppm levels of limonene [17, 19-21] which are not representative of any typical indoor concentrations. So far, only Ourrad

et al. investigated the ppb-level photocatalytic oxidation (PCO) of limonene. Authors interestingly evidenced a noticeable heterogeneous formation of SOA along limonene oxidation. However, this fundamental study was achieved in a small volume batch reactor using P25 Degussa powder photocatalyst, which remains far from any realistic indoor treatment consideration [18].

Regarding air treatment technologies, it has been shown that more than 90 % of commercialized air treatment devices in France in 2006 encompassed at least a photocatalytic stage [22]. This information highlights the high occurrence of PCO technique in air treatment devices. However, the most widespread passive air treatment technique remains adsorption for indoor purposes, as well as for more concentrated effluents. It also appears that both techniques are frequently coupled in order to minimize secondary VOC possibly released downstream the photocatalytic stage. Irrespectively of the selected air treatment process, the performances and mostly the safety of indoor treatment devices are still questionable and need to be investigated under realistic conditions. In 2009, the standard XP B 44 013 updated in 2017 in the standard NF EN 16846 [23] proposed a first protocol to characterize the efficiency of photocatalytic devices towards VOC removal in indoor environments. This standard recommends testing PCO devices versus a mixture of VOCs, namely, acetaldehyde, acetone, toluene and heptane, in a closed 1 m³ experimental chamber. Efficiencies of tested devices are compared based on their respective Clean Air Delivery Rate (CADR) values expressed in m³ hr⁻¹. CADR values are calculated as shown in Equation 1, where V is the volume of the experimental chamber (m³), k_e is the VOC decay rate in the presence of the operated photocatalytic device (expressed in h⁻¹) and k_n is the

VOC natural decay inside the experimental chamber in the absence of the photocatalytic device (expressed in h^{-1}).

Equation 1: $CADR = V \cdot (k_e - k_n)$

Nevertheless, a volume of 1 m^3 is not representative of any real indoor environment, and not compliant with recirculation air flows of commercially available air treatment devices which may be operated up to several hundreds of $\text{m}^3 \text{ hr}^{-1}$. Such discrepancies may lead to experimental biases inducing (i) misleading conclusions on tested devices and (ii) preventing any extrapolation of the performances from 1 m^3 chamber to real scale indoor environment. Moreover, the use of a small scale chamber may hinder the real impact the of air treatment process on indoor air composition and quality. Besides, in spite of the high occurrence and very specific reactivity of terpenes, no study addresses the performances and safety of commercialized air treatment devices towards the removal of these reactive VOCs under realistic indoor conditions and scale.

Thus, this work aims first to reproduce a real household action in the 40 m^3 experimental room IRINA (*Innovative Room for INdoor Air studies*) [24] using the ADOQ-50 product in order to identify and quantify VOC emissions from a real selected household product. Second, pollutant decay rates and reaction intermediates are characterized in the presence of typical and commercially available air treatment devices in order to provide a comprehensive approach of air treatment devices effective impact on indoor air chemistry and quality. This work aims at providing for the first time a real and complete

characterization of typical indoor scenario, from emission to treatment, combining unique large scale equipment with detailed and controlled physical and chemical characterizations.

2. Experimental

2.1. Experimental room: IRINA

Experiments are conducted in the 40 m³ experimental room IRINA. An accurate description and validation of this large scale and unique equipment has been proposed by Harb et al. [24]. Briefly, IRINA inner surfaces are fully covered with aluminum foils to avoid any VOC sink and source from walls. The room is operated in a semi-closed mode with a controlled air exchange rate of $\tau = 0.3 \pm 0.1 \text{ hr}^{-1}$ monitored on a three-year time-span. The air conditioning system (AC) placed in IRINA ensures temperature control as well as air homogenization. Four sensor arrays are used to continuously monitor temperature, relative humidity and CO₂ concentrations. As evidenced by Harb et al. [24], in the absence of any air treatment device in the room, the natural decay rate of each VOC in IRINA is primarily contributed by the air exchange rate of the room. Therefore it can be conveniently modeled by Equation 2 where C is the considered VOC concentration at time t (hr), C_0 is the VOC initial concentration and k_n is the pseudo-first order constant of the VOC natural decay rate.

Equation 2 : $\ln(C) = -k_n \cdot t + \ln(C_0)$

Moreover, as formerly reported in studies dedicated to VOC removal by photocatalytic or sorptive processes [25, 26], pseudo-first order heterogeneous kinetics can be considered. This kinetic is also considered by the standard NF EN 16846 [23] for autonomous photocatalytic air treatment devices; subsequently, the temporal evolution of a specific injected VOC in IRINA in the presence of a photocatalytic air treatment device is described

by Equation 3 as the convolution of pseudo first order decay rates related to (i) natural air exchange rate of the room and (ii) air treatment process.

Equation 3 : $\ln(C) = -(k_n + k_e) \cdot t + \ln(C_0)$

2.2. Analytical instruments

A description of analytical instruments coupled to IRINA experimental room is proposed in this section; complementarily, a more detailed description can be found in previous papers [24-26].

2.2.1. Gas phase analysis

VOC sampling is performed on Carbotrap 202 cartridges for 30 min using an Automated Clean Room Sampling System (ACROSS) at a flow rate of 0.20 L min⁻¹. Cartridges are desorbed using Gerstel thermal desorber. Compounds are thermally transferred under He and refocused on a cryogenic capillary trap. The gas chromatographic analysis is carried out using a 7890A type instrument from Agilent Technologies equipped with an Agilent DB-5MS chromatographic column connected to two different detectors (i) a Flame Ionization Detector (FID), and (ii) a Mass Spectrometer (MS). The typical detection limit of the FID for VOCs with abovementioned sampling conditions is 0.1 ppb.

Carbonyl VOCs are derivatized on 2,4-dinitrophenylhydrazine (DNPH) impregnated silica WATERS cartridges for 30 min at a flow rate of 2.0 L min⁻¹. Derivative hydrazones are extracted from DNPH cartridges with 3 mL acetonitrile and analyzed with Water 2487 HPLC. Compounds are eluted on a C18 column with a ternary elution program and detected by tunable wavelength UV absorption (Water 2695). Under these conditions, the typical detection limit for carbonyl compounds is 0.01 ppb.

The monitoring of CO₂ concentration is required to determine the air renewal rate of the experimental room IRINA. To that end, the concentration range to address varies from 100 ppm to 5000 ppm. Therefore, CO₂ probes based on IR absorption from KIMO are used to monitor CO₂ in IRINA as an air renewal rate tracer. The limit of detection of the CO₂ by the selected probes is 100 ppm.

Ozone concentration in IRINA is monitored using an O₃ 42M type instrument from Environnement S.A. The principle of this ozone analyzer relies on UV absorption. It provides an accurate O₃ low level monitoring in the range 0 – 10 ppm with a limit of detection determined as 0.4 ± 0.2 ppb.

2.2.2. Particle phase analysis

Particle phase data are collected every 10 min in the aerodynamic diameter range 9.82 - 414.20 nm using a Scanning Mobility Particle Sizer (SMPS) supplied by TSI. The SMPS consists in a Condensation Particle Counter (CPC) TSI 3800 coupled with a Diffusion Mobility Analyzer

(DMA). The SMPS is located in the center of the room which allows the sampling of aerosols directly from the air inside the room at a continuous flow rate of 600 mL min^{-1} .

2.3. Selection and technical specifications of air treatment devices

The purpose of this study is to address the impact of real air treatment devices on indoor air chemistry and quality. To that end, the most typical and widespread air treatment devices on the French market had to be designated. In 2015, authors inventoried twenty commercially available indoor air cleaning devices in the French market relying on (i) photocatalysis, (ii) adsorption, (iii) ionization, (iv) ozonolysis, or (v) multiple combinations of these processes. Among them, devices relying on photocatalysis and adsorption technologies or their combination are from far the most representative of the market, i.e. 95 %. Since the present study is performed in IRINA experimental room, to ensure the best compromise between (i) the volume of the experimental room, (ii) the VOC removal kinetics and (iii) realistic comfort parameters, devices with total air flow rate higher than $100 \text{ m}^3 \text{ hr}^{-1}$ have not been selected. Four devices among twenty were compliant with those criteria. The four selected devices have been tested according to the XP B 44-013 standard [27]. Devices characterized by the highest CADR have been selected for further investigations. They are named Device-1 and Device-2 in this study. Device-1 solely relies on photocatalytic oxidation while Device-2 combines adsorption with photocatalytic oxidation. Both devices have been purchased on the market, however, a detailed characterization of their design is primarily performed. Interestingly, based on the performance evaluation proposed by the standard, both devices are characterized by equivalent CADR values regarding the five model VOCs defined by the standard.

Device-1 and Device-2 are both designed with a cylindrical geometry, meaning that the photocatalytic or sorptive-photocatalytic media is shaped as a cylinder and the irradiation lamp is located along the axis of the cylinder. In both devices, the total length of the UV lamps corresponds to the length of the photocatalytic cylinder ensuring a homogeneous irradiation of the inner side of the cylindrical media. Both lamps are mercury discharges providing UVC irradiation with maximum emission bands at 254 nm. However, devices differ in terms of photocatalytic media and dimensions which impact the contact time of the treated gas with the media and the photon flux on the photocatalytic surfaces. These aspects are further detailed in the next paragraphs for each device. General scheme of the designs of both selected air treatment systems are proposed in Figure 1.

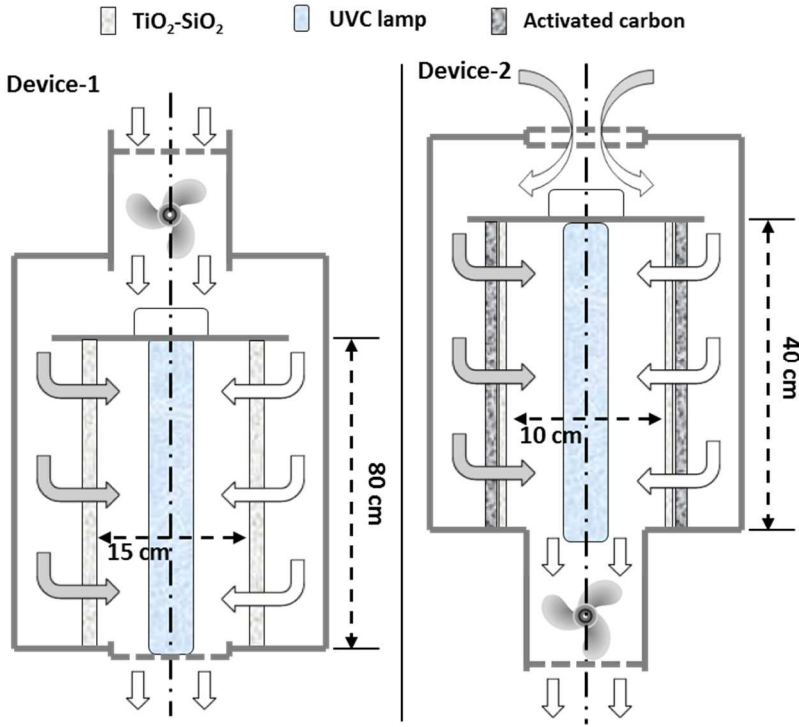


Figure 1: Schematic representations of Device-1 and Device-2

Device-1 / The photocatalytic media implemented in Device-1 is produced by Saint-Gobain and known as Quartzel [28]. The material is shaped in an 80 cm long and 15 cm inner diameter cylinder. It consists in TiO₂-coated amorphous silica fibers. The global density of that media is 100 g.m⁻² with a specific surface area of 120 m² g⁻¹; the TiO₂ load on the media is 16 g m⁻². Device-1 involves 0.4 m² of Quartzel photocatalytic media corresponding to 6.4 g of TiO₂ photocatalyst present in the device. The average total thickness of that fibrous media is 10 mm. The total flow rate of Device-1, determined with SwemaFlow, is 48 m³ hr⁻¹. Thus, assuming a homogeneous flow across the 0.4 m² photocatalytic media, the average air velocity across the media used in Device-1 is ca. 0.033 m s⁻¹ corresponding to a residence time of the treated gas in the vicinity of the 10mm-thick photocatalyst of ca. 0.3 s. The total incident UV photon flux on the inner side of the photocatalytic cylinder is 6 mW cm⁻², corresponding to a total incident power of 22.6 W. Irradiation of the media is ensured using an 80cm-long UV lamp placed on the axis of the cylindrical photocatalytic media.

Device-2 / The media used in Device-2 is a double layer 5mm-thick material. The material is shaped in a 40 cm long and 10 cm inner diameter cylinder. The total geometric surface of the media is 0.12 m². The outer layer consists in a compacted sheet of activated carbon with a density of 550 g m⁻². The inner layer of the cylinder consists in a sheet of TiO₂-coated silica fibers with a coating density of 20 g m⁻². Subsequently, the media used in Device-2 combines 66 g of activated carbon with 2.4 g of TiO₂. Considering the design of Device-2, the treated gas first flows through the activated carbon layer, then it reaches the surface of the

photocatalytic sheet. The total flow rate of Device-2 is $33 \text{ m}^3 \text{ hr}^{-1}$. Thus, assuming a homogeneous flow across the 0.12 m^2 media, the air velocity across the media used in Device-2 is ca. 0.076 m s^{-1} . This value exceeds the one of Device-1 by more than a factor 2. Considering the respective thicknesses of both layers of the media used for Device-2, residence times of the treated gas are (i) 0.05 s in the vicinity of the activated carbon layer and (ii) 0.01 s in the photocatalytic media layer vicinity. The latter value noticeably differs from Device-1 residence time by one order of magnitude. The inner photocatalytic surface of the media is directly and homogeneously irradiated with a total incident UV photon flux of 9 mW.cm^{-2} , corresponding to a total incident power of 11.1 W . Table 1 reports and compares the characteristics of Device-1 and Device-2.

Table 1: Comparative summary of the characteristics of the selected air treatment devices

	Device-1	Device-2
Material	Quartzel from Saint Gobain, 100 g m^2 of TiO_2 coated on quartz fibers	Double layer material : activated carbon + 20 g m^2 of TiO_2 coated on fibers
TiO₂ mass	6.4 g	2.4 g
Activated carbon mass	0	66 g
Total flow rate	$48 \text{ m}^3 \text{ hr}^{-1}$	$33 \text{ m}^3 \text{ hr}^{-1}$
Residence time	0.3 s	0.06 s
UV photon flux on photocatalyst surface	6 mW cm^{-2}	9 mW cm^{-2}
Total incident UV power	22.6 W	11.1 W

3. Results and discussions

3.1. Characterization of household product emissions in IRINA

In order to mimic a realistic but reproducible housecleaning action inside IRINA and the corresponding VOC emission, the following protocol has been defined. Before each housecleaning action inside IRINA, blank levels of VOCs and particles are monitored during 1 hr. Then, the housecleaning action in IRINA is performed and characterized using 20 g of ADOQ-50 product spread with a wet sponge on a 0.27 m² glass board directly placed inside IRINA. The product is leftover for 5 minutes, and then wiped using sponge and warm water in order to mimic realistic housecleaning conditions. Consecutively to the use of ADOQ-50 in IRINA, VOCs and particles are monitored inside the room for 5 hours to address their temporal dynamics consecutively to the housecleaning action.

Following any application of the housecleaning product, six terpenoid VOCs are always identified and quantified in the gas phase: d-limonene, eucalyptol, isocineole, camphene, o-cymene, and p-cymenene. Among them, only d-limonene, eucalyptol and isocineole were reported in the liquid composition of ADOQ-50 with respective masses of 2, 0.4 and 0.2 % of the total identified mass [9]. Except for VOCs listed in Table 2, it has to be mentioned that no other emitted VOC has been detected under our experimental conditions. Noticeably, no directly emitted carbonyl VOCs are detected in IRINA consecutively the household action in spite of detection limits as low as 0.01 ppb for this class of VOCs. Table 2 reports the maximum concentrations determined for the six monitored VOCs consecutively to ADOQ-50 housecleaning product emission. It can be noticed that limonene is from far the highest

emitted VOC; subsequently, this compound can be considered in the following as a relevant tracer of ADOQ-50 house cleaning product emissions.

Table 2: List of VOCs emitted from ADOQ-50 cleaning product and monitored in IRINA experimental room in the absence of any air treatment device in the experimental room, with corresponding maximum concentrations under $T = 22 \pm 1 \text{ }^\circ\text{C}$ and $\text{RH} = 50\text{-}60 \%$. Uncertainties correspond to the standard deviation between 4 similar emission experiments.

VOCs	Maximum concentrations (ppb) ($T = 22 \pm 1 \text{ }^\circ\text{C}$, $\text{RH} = 50\text{-}60 \%$)
d-limonene	38.7 ± 7.0
eucalyptol	2.0 ± 0.3
isocineole	1.9 ± 0.3
camphene	0.5 ± 0.1
o-cymene	0.6 ± 0.1
p-cymenene	0.6 ± 0.1

In order to address the impact of environmental conditions on VOC emissions from ADOQ-50, temperature and relative humidity in the experimental room have been individually varied in IRINA. First, six experiments are carried out in IRINA, with typical temperatures of indoor environments: from $18 \text{ }^\circ\text{C}$, for winter time, to $31 \text{ }^\circ\text{C}$, for summer time. During that first set of experiments, relative humidity is controlled between 50 and 60 %. Figure 2 represents maximum concentrations (ppb) of limonene emitted by ADOQ-50 housecleaning product as a function of temperature set in IRINA. The lowest emission level of limonene is found to be 15.5 ppb at a temperature of $19 \text{ }^\circ\text{C}$ while the highest (47.7 ppb) is reached at 23

°C. From 18 to 23 °C, the continuous increase of temperature enhances limonene emissions. However, at 31 °C, it can be noticed that the cleaning product dries faster on the glass plate which may therefore explain that limonene emissions get hindered, resulting in limonene maximum concentrations lowered to 30.8 ppb.

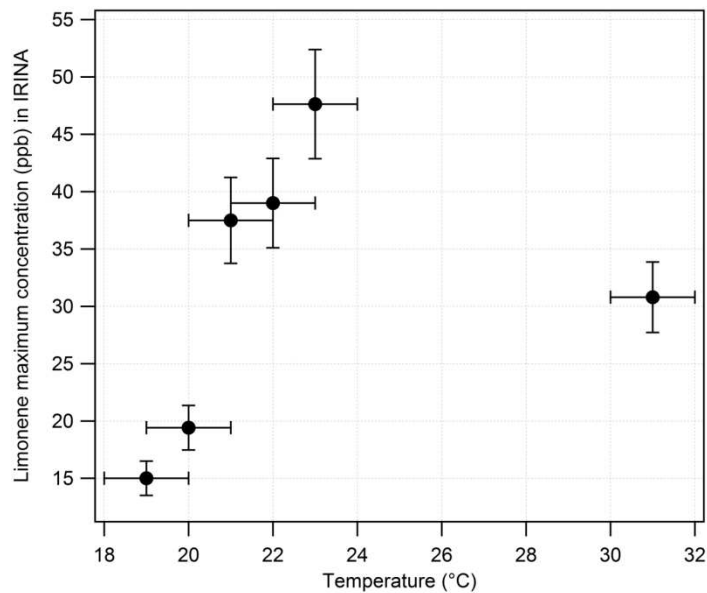


Figure 2: Evolution of limonene maximum concentration emitted from ADOQ-50 cleaning product as a function of the temperature set in IRINA experimental room (50-60 % RH). Error bars on x axis correspond to temperature standard deviation which is limited to ± 1 °C and error bars on y axis correspond to concentration measurement uncertainty which is determined as 10 %.

During the second set of experiments, the temperature in IRINA is set at 22 ± 1 °C and relative humidity is varied from 30 to 70 %. Figure 3 represents the corresponding limonene maximum concentrations (ppb) as a function relative humidity in IRINA. As it can be noticed in Figure 3, relative humidity remarkably influences limonene emission, and the maximum emission of limonene is observed around 50-55 % RH.

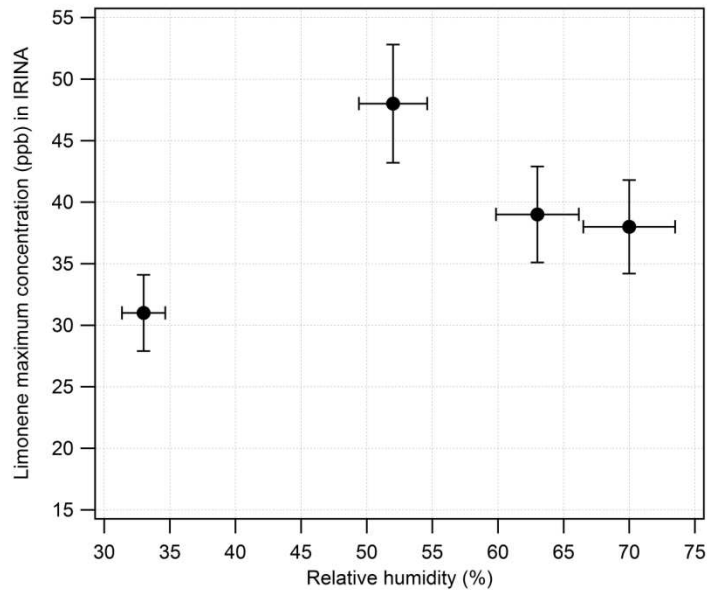


Figure 3 : Evolution of limonene maximum concentration emitted from ADOQ-50 cleaning product as a function relative humidity inside IRINA experimental room ($T\text{ }^{\circ}\text{C} = 22 \pm 1\text{ }^{\circ}\text{C}$). Error bars on x axis correspond to relative humidity (%) standard deviation which is determined as 10 % and error bars on y axis correspond to concentration measurement uncertainty determined as 10 %.

As can be retrieved from Figure 2 and Figure 3, the temperature and the relative humidity are parameters of influence on the emissions of the selected housecleaning product. The highest emissions of limonene from ADOQ-50 cleaning agent are observed under $23\text{ }^{\circ}\text{C}$ and 50-55 % RH. In order to assess the reproducibility of emissions, 4 experiments have been performed in IRINA under $22 \pm 1\text{ }^{\circ}\text{C}$ and 50 - 60 % RH; obtained results are reported in Table 1. From this table, it can be retrieved that the variation coefficients of emitted maximum concentrations are limited to 18 % between four experiments performed, thus confirming the satisfying reproducibility and control of the selected housecleaning agent emissions

inside IRINA experimental room. Under these conditions limonene maximum concentration is found to be 38.7 ± 7 ppb.

3.2. Natural decays of household product emissions in IRINA in the absence of air treatment device.

In the absence of any air treatment device, the decay of emitted VOCs is supposed to be only contributed by the air renewal rate of the experimental chamber [24]. This decay is called natural decay. An illustration of limonene natural decay profile monitored for 5 hr in IRINA consecutively to emission is presented as an insert in Figure 4. The mono-exponential profile is linearized by plotting the evolution of the logarithm of limonene concentration as a function of time (Figure 4). For this experiment, the natural decay rate of limonene is determined as 0.33 hr^{-1} . Limonene natural decay rates determined over six experiments are gathered in Figure 5 along with simultaneous CO_2 natural decay rate reported in dashed line. These six experiments were conducted over 36 days to assess the reproducibility of limonene decay rate in IRINA on a long time span.

As can be seen in Figure 5, limonene natural decay rate is characterized by a variation coefficient lower than 5 % over 6 experiments. The corresponding mean value of limonene natural decay rate in IRINA is $0.33 \pm 0.02 \text{ hr}^{-1}$. CO_2 is characterized by a mean decay rate of $0.30 \pm 0.01 \text{ hr}^{-1}$. Apart from the extraction of gaseous species due to the air renewal rate and in the absence of air treatment device, apart from air renewal rate, the natural decay rate can only get an extra contribution from a minor, but noticeable, uptake on the surfaces available in the experimental room. Indeed, limonene decay rate is slightly higher than CO_2 ,

suggesting that a minor fraction of emitted limonene is taken up onto IRINA walls. However, the contribution of this heterogeneous phenomenon to natural decay rates remains lower than 10 %. Therefore, as formerly reported for other classes of VOCs by Harb et al. in IRINA [24], these experiments confirm that limonene natural decay is chiefly contributed by the air exchange rate of the experimental room in the absence of air treatment device.

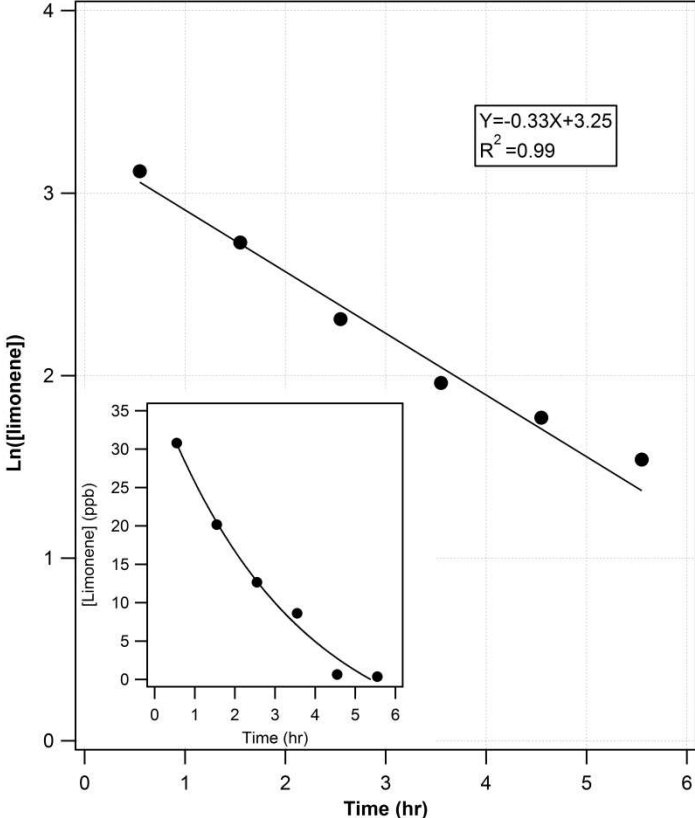


Figure 4 : Evolution of $\ln([\text{limonene}])$ as a function of time (hr) ($T^{\circ}\text{C} = 22 \pm 1^{\circ}\text{C}$; RH=50-60%).

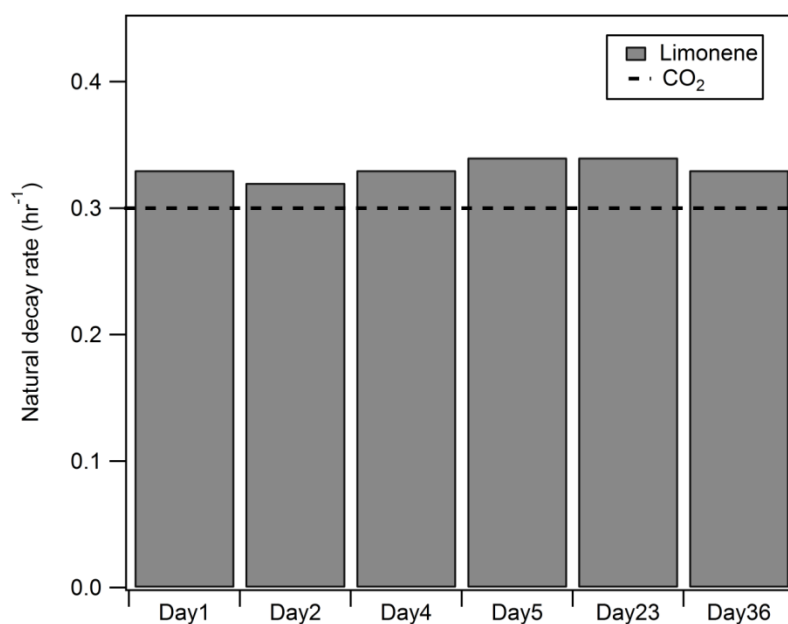


Figure 5 : Comparison of limonene natural decay rates with CO₂ decay rates (T°C = 22 ± 1 °C; RH = 50 - 60 %)

3.3. Decay rates of household product emissions under treatment.

Similarly to most of the air treatment devices available on the market, Device-1 and Device-2 combine different processes that may impact the removal decay of limonene used as a tracer of the household product emissions: (i) adsorption on the media, (ii) direct UVC photolysis, (iii) indirect ozonolysis by UVC-generated O₃ and (iv) photocatalysis. In order to discriminate the contributions of these processes on limonene removal, different sets of experiments have been carried out: (i) processing of the VOC solely in the presence of the media, i.e. without any UV irradiation, (ii) evaluation of O₃ production by UVC, (iii) evaluation of ozonolytical process and (iii) global decays of VOCs while devices are fully operated, i.e. media and UVC.

Contribution of the adsorption on the media to limonene removal

First, UVC lamps have been disconnected to prevent any photonic activation of the media and the gas phase species and each device has been operated in the experimental room IRINA consecutively to household product emission. The purpose of that set of experiments is to assess the impact of the sorption process onto the media on the decay of emitted tracer VOC. Obtained results are referred to as “media only” experiments. Decay rates of limonene monitored under these conditions are 0.38 hr^{-1} and 0.56 hr^{-1} respectively for Device-1 and Device-2. Considering that the natural decay rate of limonene is determined as 0.33 hr^{-1} , respective contributions of sorptive processes are 0.05 hr^{-1} for Device-1 and 0.23 hr^{-1} for Device-2. It clearly appears that sorption processes contribute to the removal of limonene in the absence of irradiation. The media used in Device-2 induces the highest uptake of limonene. It is coherent with the nature of that media since it encompasses a 66 g activated carbon layer. However, the sorptive properties of Quartzel media used in Device-1 are noticeable and are clearly appraised under our experimental conditions. Respective contributions of natural decays and adsorption decays are displayed in Figure 7 for the “media only” experiments.

Considering that the sorptive layer present in Device-2 induces a significant contribution on limonene removal and is dissociated from the oxidative photocatalytic layer, the sorptive removal capacity of Device-2 has been addressed on multiple and consecutive household product emissions. To that end, six consecutive emissions of the ADOQ-50 product were performed along three days with two emissions per day. Interestingly, the removal of

limonene by Device-2 along these “media only” experiments remained constant with 0.23 hr^{-1} for each and no subsequent release of limonene. This results suggest a significant adsorption capacity of the media used in Device-2 compared to the amount of limonene released along the emission experiments. This behavior is supported by the works of Metts and Batterman [29] and Sidheswaran et al. [30], authors report total sorptive capacities for terpene and C_{11} VOCs onto various activated carbons in the 10 mg.g^{-1} range under indoor conditions. As a consequence, the total amount of limonene emitted by a single housecleaning emission would require less than 1 % of the uptake capacity of the activated carbon layer from Device-2. Thus, in the context of the present study, the sorptive contribution of Device-2 regarding the removal of transient limonene concentration peaks is constant along the various emissions. However, the presence of sorptive material, even in contact with photocatalytic layers, definitely questions their lifetimes and the subsequent release of VOCs on long term use.

Evaluation of photo-activated processes induced by UVC

Second, the use of UVC lamps for photocatalytic media activation definitely questions (i) the production of ozone in indoor environment, (ii) the direct photolysis of limonene and (iii) the contribution of ozone to the removal process of limonene. This issue is firstly addressed in the absence of any emitted VOCs in the room. The formation of O_3 by each device has been assessed under two configurations: first, with the media inserted in the devices; second, without any media inserted in the devices. Temporal profiles of ozone contributed by devices under both configurations are reported in Figure 6. All along the experiments dedicated to O_3 characterization, $3 \pm 1 \text{ ppb}$ of O_3 have been monitored in the experimental

room under steady state conditions. This background level was subtracted from O_3 concentration monitored in the presence of the treatment devices to emphasize their respective contributions to O_3 level as reported on Figure 6.

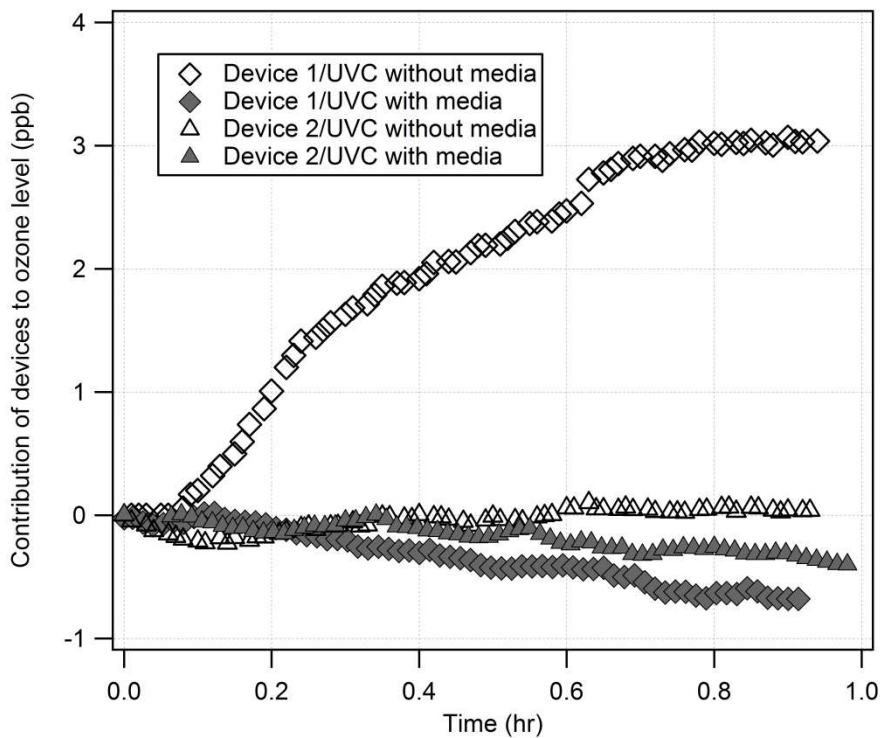


Figure 6 : Evolution of ozone produced by Device-1 (diamond symbols) and Device-2 (triangle symbols) in IRINA experimental room as a function of time; $t = 0$ hr corresponds to the startup of devices; UVC lamps of devices are on, but devices are operated either with media (full symbols) or without media (empty symbols).

In the absence of media, the operation of Device-1 induces an increase in ozone concentration in IRINA reaching a ca. 3 ppb steady state level. The photolysis of O_2 from ambient air by the UV lamp of Device-1 is at the origin of the formation of ozone. The absorption cross section of O_2 indicates that its photolysis requires wavelengths lower than

220 nm. The emission spectrum of UVC lamps used in Device-1 as well as Device-2 are characterized by a broad emission band centered at 254 nm in the UVC range. Thus, the formation of ozone from the photolysis of O₂ is induced by minor emissions in the foot of the main emission band, i.e. with wavelengths shorter than 220 nm. Considering the natural air renewal rate of IRINA and the increase in O₃ concentration, UVC lamps of Device-1 subsequently produce 1.7×10^{-6} μmol hr⁻¹ of ozone (i.e. 79.0 μg hr⁻¹) in the steady state regime. Interestingly, it can be noticed on Figure 6 that ozone is not released anymore in the experimental room as Device-1 is operated in the presence of its photocatalytic media. This behavior can be correlated with the ability of irradiated TiO₂-based photocatalyst to promote ozone decomposition; this phenomenon has been reported by Ohtani et al. [31] and it can be suggested that it contributes to the slight decrease of ozone level in IRINA as full Device-1 is operated. As a consequence, under UVC irradiation and in the presence of the media, the oxidation process taking place in Device-1 can be considered as ozone-assisted photocatalysis; UVC produced ozone get decomposed onto the irradiated photocatalytic media which may enhance the heterogeneous photocatalytic oxidation process. It should be mentioned that ozone concentration in the vicinity of UVC lamps inside Device-1 is locally higher than the concentration of ozone monitored in the experimental, i.e. once buffered by the 40 m³ volume and the air renewal rate.

The question of direct photolysis of limonene in the presence of minor but energetic wavelengths lower than 220 nm emitted from UVC lamps can be addressed considering the work of Smialek et al.[32]. Authors evidenced that the absorption cross section of limonene is negligible for wavelengths higher than 200 nm. As a consequence, the overlapping

between the emission band of the UV lamp centered at 254 nm and the absorption cross section of limonene appears as a non-contributive process in the removal of limonene.

In spite of the fact that Device-2 uses UVC lamps with the same emission spectra than Device-1, no impact of Device-2 on O₃ concentration in IRINA is noticeable in the absence of the media. This contrasted behavior can be related to (i) the lower power of UVC lamps used in Device 2, and (ii) the shorter residence time of processed air in the UVC irradiated zone in Device-2 (1.6 s) compared to Device-1 (4.8 s), thus hindering ozone formation. Similarly, no contribution of Device-2 to ozone level in IRINA can be noticed in the presence of the media. Subsequently, the oxidative capacity of Device-2 mostly proceeds from TiO₂ photocatalyst activation without any enhancement by O₃.

It can be noted in Figure 6 that the concentration profiles of ozone in the presence of media in Device-1 and in Device-2 are both characterized by a slight but noticeable decreasing trend. This behavior suggest that beyond the removal of ozone produced by Device-1, media may induce a decrease in residual ozone concentration in the experimental room.

Contribution of ozonolysis to the removal of limonene

In order to address the role of ozone produced by UVC on the removal of emitted limonene, emissions of household products have been successively treated using Device-1 and Device-2 in the absence of their respective media. Determined limonene decays under these conditions are 0.39 hr⁻¹ for Device-1 and 0.30 hr⁻¹ for Device-2. The absence of media implies no sorptive removal of limonene. Moreover, the direct photolytic removal of limonene can be ruled out. Subsequently, the global decay of limonene in that set of experiment can only

be contributed by (i) the natural air exchange rate and (ii) the removal of limonene by ozone produced. Indeed, ozonolysis is a major oxidation route of terpenes, it is characterized by high homogeneous [15, 16] and heterogeneous reaction rates [33].

Considering that 3 ppb of O_3 are continuously produced by Device-1 under our experimental conditions (Figure 5), the decay of limonene observed in the presence of that device can be decomposed as (i) 0.33 hr^{-1} related to limonene natural decay rate and (ii) 0.06 hr^{-1} related to limonene ozonolysis. In the case of Device-2 the decay of limonene directly corresponds to its natural decay. This behavior confirms that insignificant levels of ozone are produced by Device-2 without media and no quantifiable ozonolysis of limonene occurs using that device. The respective contributions of the discussed phenomena are reported in Figure 7, where the corresponding sets of experiments are referred to as “UVC only”.

Limonene removal by complete air treatment devices

Finally, Device-1 and Device-2 are successively placed in IRINA to assess their global impact on the removal of limonene emitted from ADOQ-50 cleaning product. In that set of experiments, the air treatment devices are fully operated, meaning that media are present in the devices and UVC lamps are operated. Obtained results are reported in Figure 7 and referred to as “complete treatment”. Respective decays of limonene are $1.79 \pm 0.04 \text{ hr}^{-1}$ and $0.69 \pm 0.04 \text{ hr}^{-1}$ for Device-1 and Device-2. Device-1 provides a complete removal of primary emitted VOCs within 40 minutes. Similarly to former sets of experiments in IRINA, both decays are contributed by 0.33 hr^{-1} corresponding to limonene natural decay rate (Figure 6). Note that the calculations made to determine the various decay rate of each contributive

removal process assume a first order kinetic. This point is supported by the mono-exponential decay profiles of limonene treated under the various experimental configurations.

Considering that sorption is a preliminary step of any photocatalytic process and that in the case of Device-1 the sorptive process solely occurs onto the photocatalytically active media, this contribution cannot be discriminated from the photocatalytic treatment of limonene. Similarly, as evidenced on Figure 5, UVC-produced ozone is photocatalytically decomposed and contributes to the photocatalytic removal of limonene. As a consequence, the decay of limonene treated by Device-1 is contributed up to $1.46 \pm 0.04 \text{ hr}^{-1}$ by the photocatalytic processing of limonene.

In contrast, the sorptive removal of limonene treated by Device-2 is mostly contributed by the activated carbon layer that does not directly contribute to photocatalysis unless diffusion of sorbed species to the photocatalyst. Nevertheless, such diffusion phenomena are not clearly evidenced and contributions of sorbent and photocatalyst tend to remain uncorrelated. Thus, limonene sorptive decay is proposed to be differentiated from photocatalytic decay in the case of Device-2 treatment. Moreover, the ozonolytical pathway has been evidenced as insignificant using Device-2. Therefore, the decay of limonene treated by Device-2 is proposed to be parted into (i) $0.23 \pm 0.01 \text{ hr}^{-1}$ related to the adsorption onto activated carbon and (ii) $0.13 \pm 0.03 \text{ hr}^{-1}$ related to photocatalysis. When compared to Device-1, Device-2 appears as a weakly oxidative system since more than 62 % of the observed decay is provided by a non-reactive process. Moreover, its photocatalytic contribution is evaluated as 7.5 times lower than Device-1. Interestingly, Harb et al.

investigated the removal of VOCs emitted from wood based materials using the same air treatment devices in IRINA experimental room. Major emitted VOCs from wood based materials are terpenes and limonene is one of the predominant emitted terpenes [34]. Similarly authors reported contrasted behaviors between Device-1 and Device-2: limonene conversion rate reached 40 % using Device-2 while it exceeded 80 % using Device-1. These results confirms the weaker removal performances of Device-2 compared to Device-1 when operated under real scale environments. This aspect is investigated in a deeper way in the section related to reaction products.

It clearly appears that two air treatment devices commercialized with close technical specifications and characterized by equivalent performances according to current standards [23] provide unexpectedly contrasted removals of emitted limonene at real scale in terms of (i) removal pathways (adsorption, ozonolysis, and photocatalysis) and (ii) removal kinetics. Global decay rates related to device actions differ by a factor 4 and photocatalytic decays differ by a factor 7.5. These behaviors were not discriminated or even addressed by current standards available for photocatalytic device evaluation. These results clearly question the advancement of the oxidation processes and subsequently the formation of reaction products.

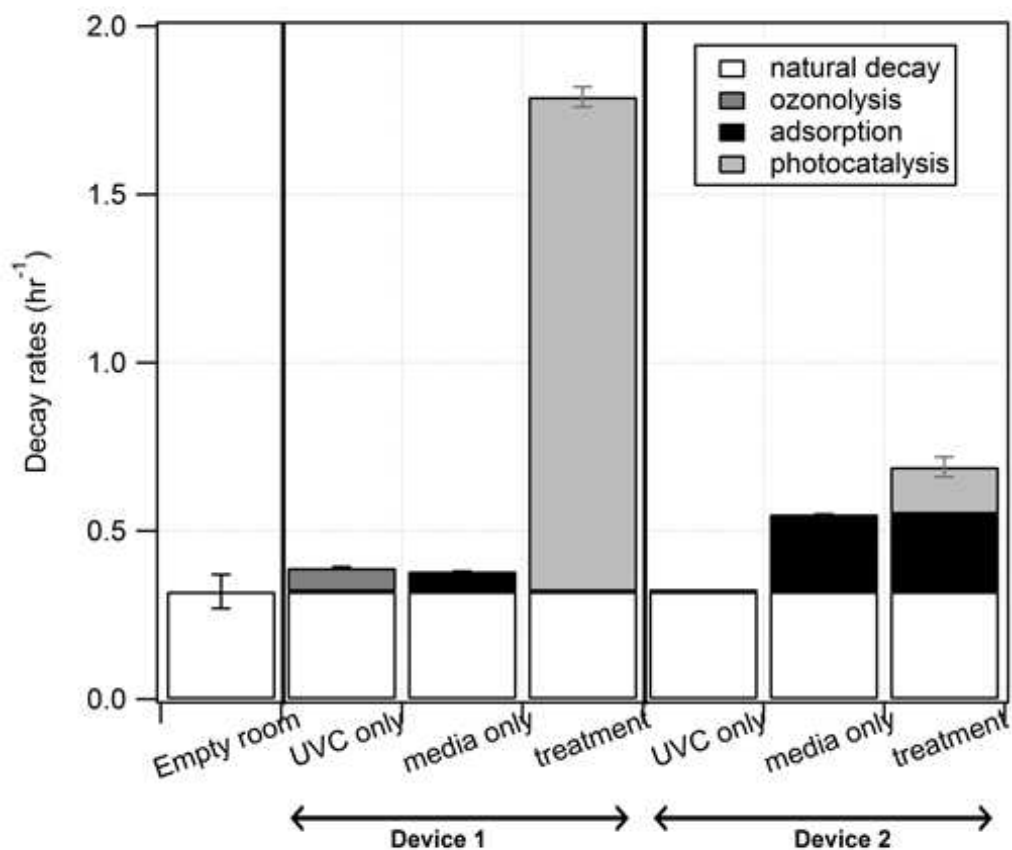


Figure 7 : Decay rates of limonene determined in IRINA experimental room in the absence of any air treatment device (*empty room*) and in the presence of each selected device (*DEVICE-1* and *DEVICE-2*). Air treatment devices are operated (i) with UVC only and no media (*UVC only*), (ii) with media only and no UVC (*media only*) and (iii) with UVC irradiated media (*complete treatment*).

(T°C= 22 ± 1°C; RH=50-60%)

3.4. Reaction products

An inclusive characterization of gaseous and particulate by-products produced during the treatments of VOCs emitted by the household product in the presence of both devices is performed. In addition, the evolution of the device performances with time is evaluated

along a continuous 10-hour operation. Two approaches are proposed: (i) treatment of emitted VOCs right after the device is turned on, so called “at startup” experiments and (ii) treatment of emitted VOCs after the device has been operated for 8 hours, so-called “after 8 hours of operation” experiments. The quantification of gaseous by-products formed along the removal of limonene makes possible the determination of the contributions of by-product to the process carbon mass balance.

Gas phase reaction products / Device-1

Figure 8 (a) represents the temporal profiles of the gaseous products monitored during the treatment of household product emissions in IRINA at startup of Device 1. As shown in this figure, a total of six carbonyl VOCs are identified and quantified in the gas phase. Formaldehyde, acetaldehyde and acetone are the major by-products with respective maximum concentrations of 31, 22 and 12 ppb reached within 0.5 hour of treatment. This experiment evidences that Device-1 transiently converts ca. 40 ppb of emitted limonene into ca. 30 ppb of formaldehyde which is more impacting regarding indoor air quality. However, formaldehyde is completely removed from the experimental room after 2 hours of treatment.

The contribution of the reaction products to the carbon mass balance during the treatment of limonene by Device-1 at start-up are reported in Figure 9 (a). Calculations of carbon mass balances are based on limonene initial concentration and encompass its natural decay during the experiment. As can be noticed in Figure 9, the contribution of organic compounds identified and quantified in the gas phase ranges from 8.8 % to 33 % of the carbon mass

balance and may subsequently impact indoor air quality. The maximum value is reached after 0.5 hour of treatment, correspondingly to the massive initial formation of lighter carbonyls in the presence of Device-1.

Since Device-1 treatment solely relies on a photocatalytic process, its carbon mass balance can be compared to similar calculations performed by Ourrad et al. [18] for limonene photocatalytic oxidation. The 33 % contribution of gaseous reaction products is higher in the case of realistic indoor conditions compared to the lab scale study of Ourrad et al. [18] who reported 12 % as the highest contribution. This difference could mainly be enlightened by the residence time of limonene in contact with the photocatalyst. Indeed, Device-1 operates at a flow rate of $48 \text{ m}^3 \text{ hr}^{-1}$, thus the ratio between the operation flow rate of the device and the volume of IRINA is equal to 1.2 hr^{-1} . Moreover, the residence time of limonene in contact with the photocatalyst is limited to 0.3 s, while it was quasi infinite in the batch reactor configuration of Ourrad et al. [18]. Therefore the oxidation process in the study of Ourrad et al. is probably more advanced which leads to a lower formation of by-products. As a result, the assessment of photocatalytic processes onto indoor air quality cannot be extrapolated from lab scale experiments, but requires real scale equipment and protocols.

After 8 hours of continuous operation of Device-1, the emission protocol of household product is performed in the experimental room for a second time. In Figure 8 (b) and (d) the time is referenced on the second emission procedure, i.e. at $t=0 \text{ hr}$. Only 4 carbonyl VOCs are detected during the treatment of emitted VOCs by Device-1 (Figure 8 (b)). Formaldehyde, acetaldehyde and acetone are still the major by-products. Interestingly, their respective maximum concentrations only reach 9, 4 and 7 ppb within 1 hour of treatment

which is less impacting regarding indoor air quality. The corresponding contribution of gas phase reaction products reaches a maximum of 16.5 % (Figure 9 (b)). Thus, not only the diversity of emitted by-products decreases with operation time, but also their concentrations and contributions to the carbon mass balance. Limonene removal decay noticeably remains the same with a variation lower than 5 % between measurements performed at startup and after 8 hours of operation. This result suggests that, at start-up, Device-1 not only treats the pollution peak, but also probably regenerates its photocatalytic media where VOCs from ambient background may have been accumulated while waiting for experiment start-up. Thereby, Device-1 gains in performances regarding oxidation reaction advancement and gaseous by-product formation after several hours of photocatalytic operation acting as a self-cleaning of that device. This behavior definitely questions the relevance and representativeness of evaluating photocatalytic air treatment devices at start-up or after several hours of operation.

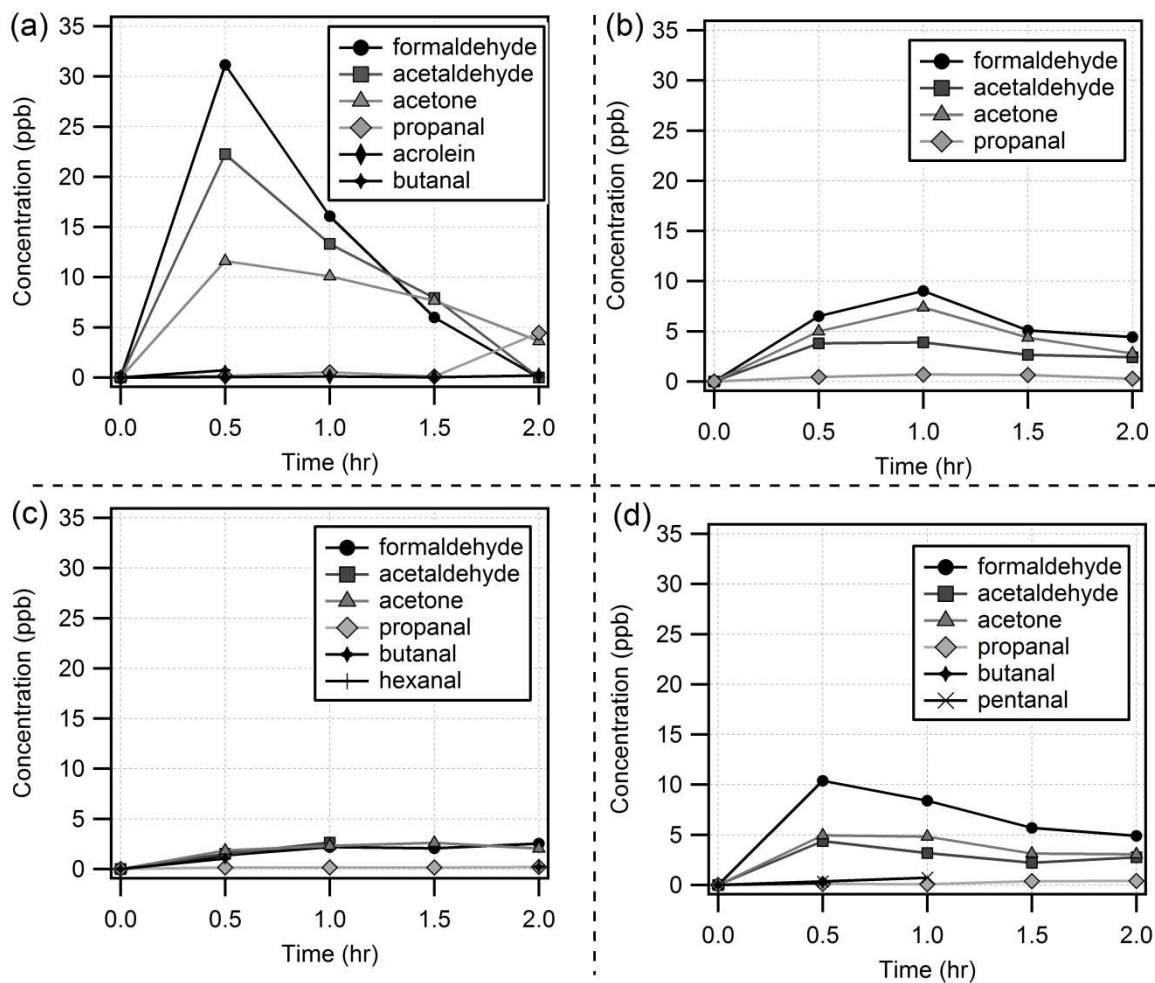


Figure 8 : Temporal profiles of the gas phase reaction intermediates monitored during the treatments of household product emissions in IRINA using Device-1 ((a) at startup and (b) after 8 h of operation) and using Device 2 ((c) at startup and (d) after 8 h of operation), $T^{\circ}C = 22 \pm 1^{\circ}C$; RH = 50-60 %. NB: in (a) and (c) the first emission of household product is performed at $t=0$ hr; in (b) and (d) the second emission of household product is performed at $t=0$ hr. NB: the uncertainties on monitored VOC concentrations are lower than 10 %.

Gas phase reaction products / Device-2

In the presence of Device-2, six carbonyl VOCs are identified and quantified in the gas phase during the “at startup” experiment (Figure 8 (c)). Except acrolein and hexanal, the diversity of gas phase products is equivalent regarding major intermediates for Device-1 and Device-2. Unlike Device-1, when Device-2 is operated, concentrations of gas phase products remain lower than 2.5 ppb. This result can be correlated with the fact that limonene photocatalytic removal using this device is 7.5 times lower than Device-1 (section 3.3.). In accordance with limited gas phase intermediate concentrations, the contribution of products to the carbon mass balance is lower than 6.2 % after 1 hour of treatment. Therefore, Device-2 does not significantly impact indoor air quality regarding side-product generation, but its primary VOC removal ability remains consistently limited.

Beyond 8 hours of operation (Figure 8(d)), concentrations of reaction products are noticeably higher as the second household product emission is performed. Compared to “at startup” experiments, formaldehyde and acetaldehyde maximum concentrations are respectively superior by factors 4 and 2, and the maximum contribution of gaseous products to the carbon mass balance reaches 16 % (Figure 9 (d)). Since the sorptive capacity of Device-2 remains constant along consecutive emissions on that time range, as mentioned in section 3.2, the decrease of the performances related to the release of reaction products is suggested to be induced by photocatalytic media deactivation. Surface extractions and analyses would be required to address that hypothesis. However, this behavior suggests that the sorptive layer present in Device-2 does not show any significant contribution to prevent secondary VOC release in the environment.

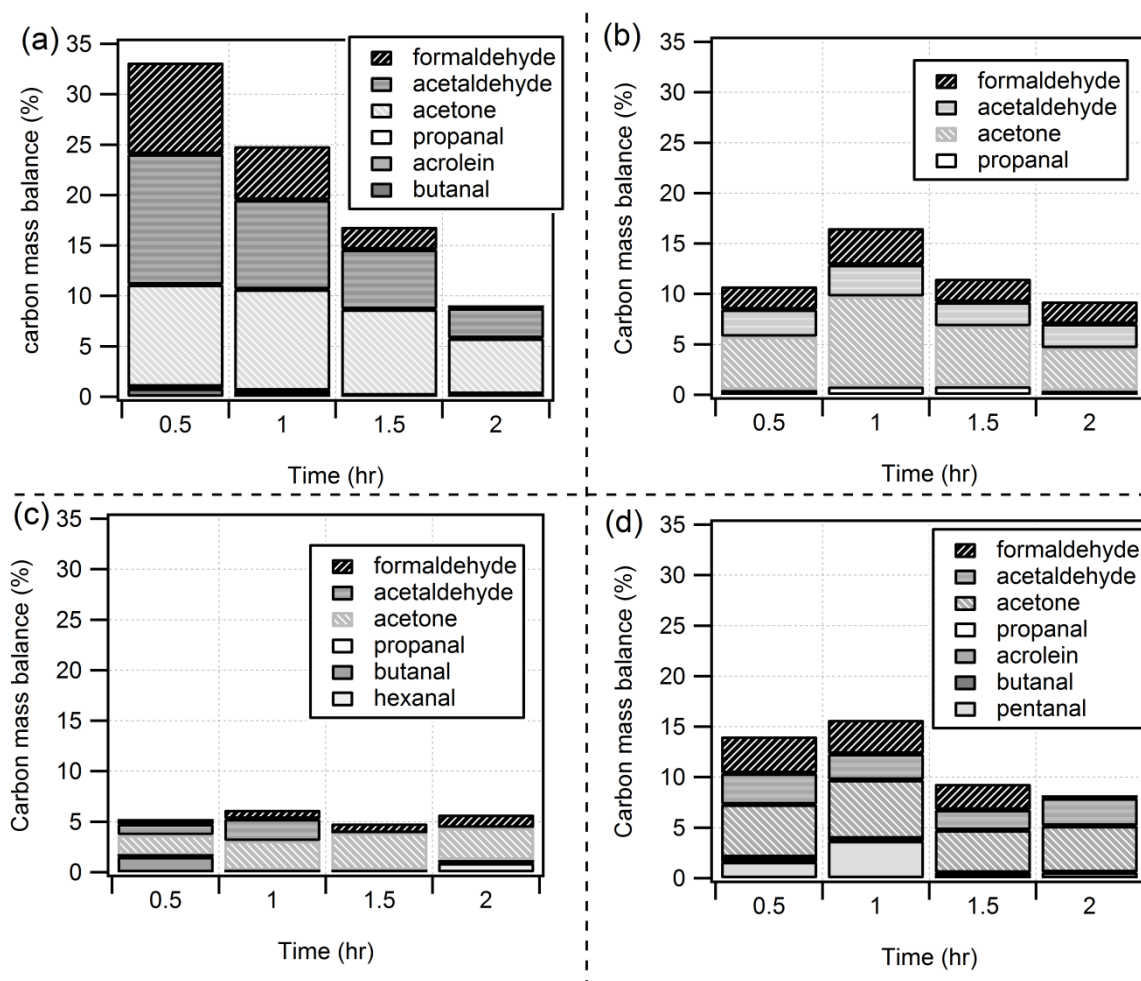


Figure 9 : Contributions of the gaseous reaction products to the carbon mass balance as a function of time during the photocatalytic oxidation of ADOQ-50 emitted limonene in IRINA using Device 1 ((a) at startup and (b) after 8h of operation) and Device 2 ((c) at startup and (d) after 8h of operation) ($T^{\circ}\text{C} = 22 \pm 1^{\circ}\text{C}$; RH = 50-60 %).

Characterization of secondary organic aerosol (SOA) formation

In 2015, Ourrad et al. [18] evidenced for the first time that the photocatalytic oxidation of limonene at ppb levels possibly leads to the formation of SOA. However, these observations were obtained in a static batch photocatalytic reactor with several hundreds of ppb of

limonene. Thus, SOA generation by a dynamic high flow photocatalytic device with relatively low concentrations of limonene and inside large volume chamber remained an open question. In order to address this crucial indoor air quality aspect, particulate phase monitoring during the treatments of housecleaning product emissions with both devices was first performed. Before switching on the devices 2000 ± 500 particles cm^{-3} are monitored as steady background concentration of particles. This level is in accordance with formerly reported data related to the validation IRINA [24].

Second, background levels of particles are monitored for one hour in the presence of both devices to assess the impact of their respective air flows on the background particle level in IRINA. Results of the background number of particles both in the presence and in the absence of air purifiers are presented in Table 2. As reported in this figure, the variation of the number of particles in IRINA remains within the measurement uncertainties in the absence of any VOC, thereby device operations do not lead to any significant resuspension and do not noticeably impact the background levels of particles.

Table 3 : Background levels of number of particles in IRINA both in presence and in absence of photocatalytic devices, error bars correspond to the standard deviation of the number of particles monitored over a 1 hour time span, no VOC is introduced in the experimental room under these experiments.

	Particle background level in IRINA (.cm^3)
No device & no VOC	2000 ± 500
In the presence of Device-1 (but no VOC)	2134 ± 236
In the presence of Device-2 (but no VOC)	2105 ± 406

The evolution of the number of particles as a function of time during the treatment of VOCs emitted by household product using both devices, at startup, is shown in Figure 10 along with mean background level of particles (grey dashed line) and background variation zone (dashed rectangle) in IRINA. As can be seen in Figure 10, no significant variation of the number of particles in IRINA is detected during the treatment of emitted VOCs using Device-1. Observed variations remain within the typical variability of the background level of particles. However, when Device-2 is operated in IRINA for emission treatment, particulate formation is significantly observed with maximum generated particles of 5300 particles cm^{-3} above background level reached 0.35 hr after treatment startup. Particulate by-products formation number decreases and reaches a stabilized level of 1300 particles cm^{-3} above background level after 5 hr of treatment.

As reported on Table 2, the background number of particle measured when Device-2 is turned on did not show any increasing trend in the absence of limonene, thereby generated particles could neither be due to resuspension of existing particles in IRINA nor to particles emitted by the device itself (TiO_2 particles, silica particles, activated carbon particles, etc...). Generated aerosols are effectively related to the photocatalytic conversion of emitted limonene in IRINA. Subsequently, the formation of SOA induced by a photocatalytic process is verified under realistic indoor air conditions.

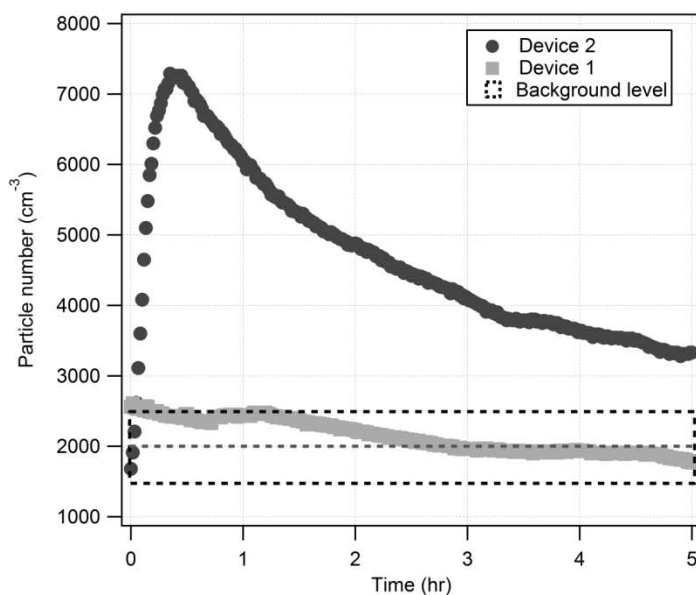


Figure 10 : Temporal evolutions of the number of particles during the treatment of household product emissions in IRINA using Device-1 and Device-2 ($T = 22 \pm 1$ °C; RH = 50-60 %). The mean background level and the background variation zone are respectively marked with a dashed grey line and dashed black rectangle.

The size distribution of SOA formed by Device 2 is obtained by connecting a DMA upstream the CPC and sampling the air inside IRINA every 10 minutes (Figure 10 (a)). Obtained profiles show a particle modal diameter shifting from 14.1 nm after 0.23 hr to 38.5 nm when the maximum number concentration is reached (i.e. almost at 1 hr of treatment) and further to 47.8 nm after 2hr of treatment (Figure 10 (b)). The decrease in the number of particles and increase in their diameters are expected tendencies and can be explained by the condensation of SOA leading to aerosols with larger modal diameter. These measurements make possible the evaluation of the total aerosol mass concentration which is later used to calculate SOA contributions to the carbon mass balance of the oxidation process and assess their impact on indoor air quality.

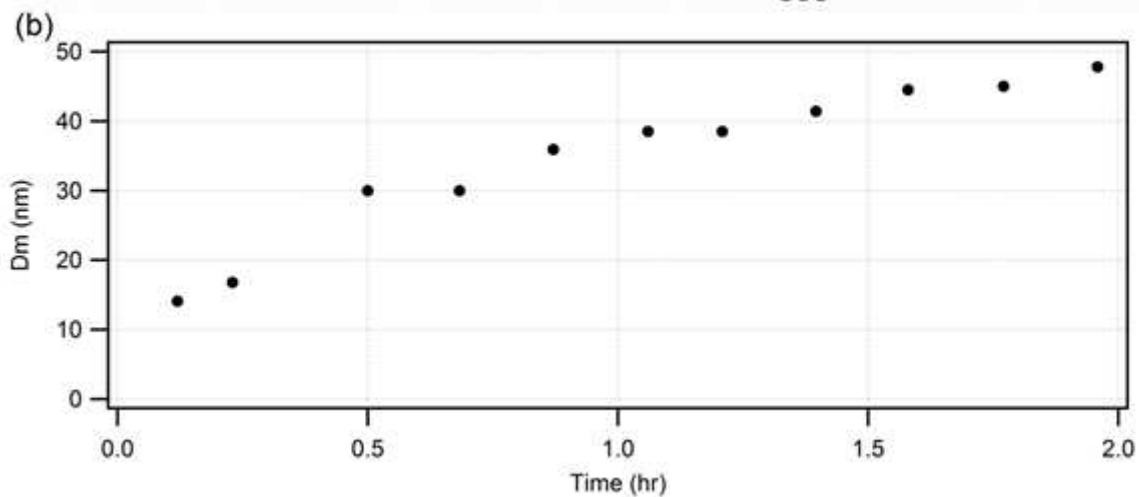
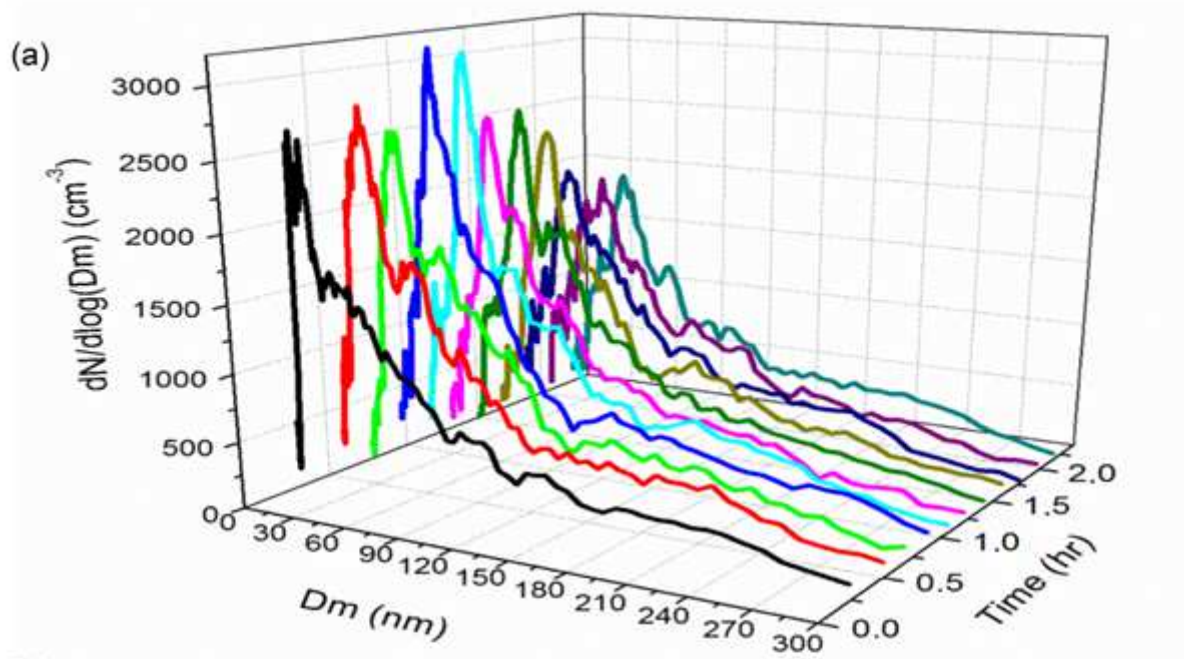


Figure 11 : (a) Evolution of SOA size distribution during the photocatalytic oxidation of ADOQ-50 emissions in IRINA using Device 2 ($T^{\circ}\text{C}= 22 \pm 1^{\circ}\text{C}$; $\text{RH}=50\text{-}60\%$). (b) Evolution of particle modal diameter during the photocatalytic oxidation of limonene emitted from ADOQ-50 in IRINA using Device 2.

Based on SMPS size distribution measurements, SOA mass concentration is calculated assuming spherical particles with a density of 1.25 g cm^{-3} [35, 36]. Figure 11 shows the aerosol mass concentrations as a function of time. As can be seen in this figure, obtained SOA mass concentrations are low and do not exceed $2.6 \mu\text{g m}^{-3}$. These mass concentrations

are first corrected taking into account the air exchange rate of the room, 0.30 hr^{-1} , which acts as a dilution effect. The dilution factor was calculated at each point and ranged between 7 and 58 % respectively for 0.23 hr and 2.0 hr. Once the air exchange rate is taken into account, the room is considered to have no leakage points, thus the remaining particle decrease is considered as due to wall losses in IRINA that can be corrected assuming a first order loss rate onto walls. This loss rate is assumed to be independent of the particles size [18, 37, 38]. Only data points after new particle formation stops are taken into account, i.e. beyond 1.5 hr of treatment. The loss rate constant, k_{loss} , is calculated using Equation 4 where $M(t)$ is the aerosol mass concentration measured at time t and corrected for dilution and C a constant.

Equation 4 : $\ln M(t) = -k_{\text{loss}} \cdot t + C$

The slope of the linear fit leads to a value of $k_{\text{loss}} = 0.109 \text{ hr}^{-1}$. Obtained k_{loss} value is significantly higher than previously reported value by Ourrad et al. [18]. Interestingly, the surface to volume ratio (S/V) of IRINA ($1.71 \text{ m}^2 \text{ m}^{-3}$) is at least 20 times lower than the S/V ratio of the reactor ($35,33 \text{ m}^2 \text{ m}^{-3}$) used by Ourrad et al. to conduct their experiments. However, the higher wall loss phenomenon in our experimental conditions can be explained (i) by the fact that the homogenization in IRINA is ensured using an AC to promote air mixing, thus air dynamic in IRINA is more important compared to a static batch reactor, thereby the contact between particles and wall surfaces is enhanced, and (ii) by the fact that the homogenization is ensured by recirculation through AC system which makes possible the particles uptake on the AC fans.

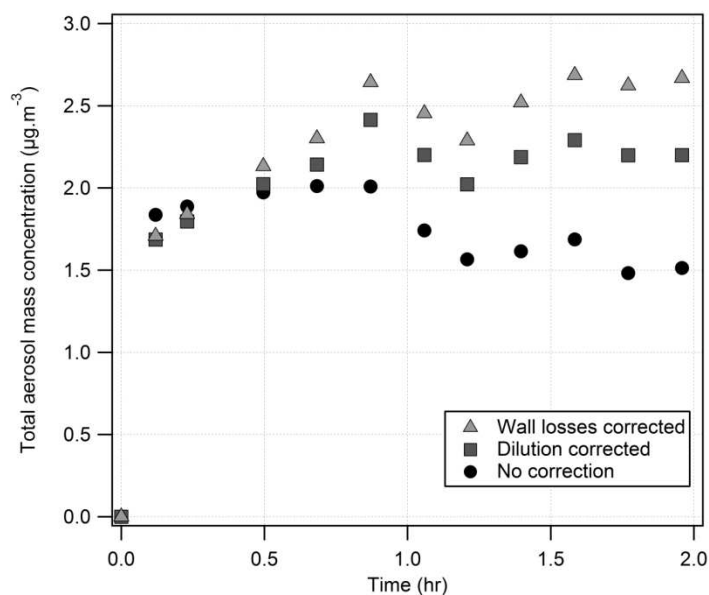


Figure 12 : Aerosol mass concentrations measured during the photocatalytic oxidation of ADOQ-50 emitted limonene in IRINA using Device 2 as a function of time, after dilution correction and wall losses correction ($T = 22 \pm 1^\circ\text{C}$; $\text{RH} = 50\text{-}60\%$).

To assess the contribution of generated SOA to the carbon mass balance of VOC emission treatment by Device 2, the number of carbon atoms involved in SOA per m^3 is calculated considering a ratio of organic matter to organic carbon of 1.6 [39-41]. The contribution of SOA to the carbon mass balance of Device-2 treatment does not exceed 0.03%. Thus, under our experimental conditions the impact of SOA on indoor air quality remains insignificant. However, it is important to mention that in our case only one cleaning product is used thus emitted concentrations are low compared to a complete housekeeping action involving different cleaning products; as a consequence deeper investigations of SOA formation by oxidation indoor air treatment device should be performed in order to confirm the limited impact of organic nanoparticles release on indoor air quality.

3.5. Carbon mass balances

Figure 12 presents an overview of the reaction carbon mass balance over 2 hours of treatment. It shows the respective contributions of limonene, gaseous and particles by-products at startup (a and c) and after 8 h of operation (b and d) for both devices. Under our experimental conditions and considering analytical instruments used to characterize the gas phase in IRINA, limonene mineralization into CO and CO₂ cannot be directly monitored due to CO₂ concentration of ca. 400 ppm in IRINA. However, it is assumed that the unidentified fraction of the carbon mass balance is primarily contributed by CO₂.

Within 2 hours of treatment, 94 % of limonene is removed when Device 1 operates at startup. While after 8 hr of operation the removal reaches almost 99% for the same duration treatment. Thus Device-1 performances are improved both in limonene removal and by-product formation after 8 hr of operation. On the other hand, with Device-2, after 2 hr of treatment only 57 % and 55 % of limonene is removed respectively at startup and after 8 hr of operation. Thus Device-2 performances remain limited regarding limonene removal.

The faster removal of primary emitted limonene by Device-1 and the higher contribution of oxygenated reaction products with low molecular weights attest of the higher oxidative ability of that device. In contrast, the limited removal of emitted limonene by Device-2 and the low contribution of gas phase reaction products to the carbon mass balance evidence a weaker oxidative capacity of that second device. The low conversion of limonene and the weak contribution of lighter oxygenated VOCs in the carbon balance suggest a limited

advancement of the oxidation process induced by Device-2. Considering that SOA formation from limonene results from the partial oxidation of limonene molecules leading to coagulation of oxidation products and not to limonene degradation, the production of SOA by Device-2 attest of a weakly oxidative process. As a consequence carbon mass balances reported in Figure 12 illustrate the respective advantages and drawbacks of each device as well as their contrasted impact on indoor air quality from primary VOC removal as well as side product formation point of views.

Device-1, solely relying on photocatalytic oxidation technology, showed higher global efficiency than Device-2 combining photocatalysis with adsorption. Therefore, combining photocatalysis to other technologies does not seem to be as efficient as focusing solely on photocatalysis and optimizing all possible parameters such as device dimensions, irradiation source, surface of photocatalyst and flow rate.

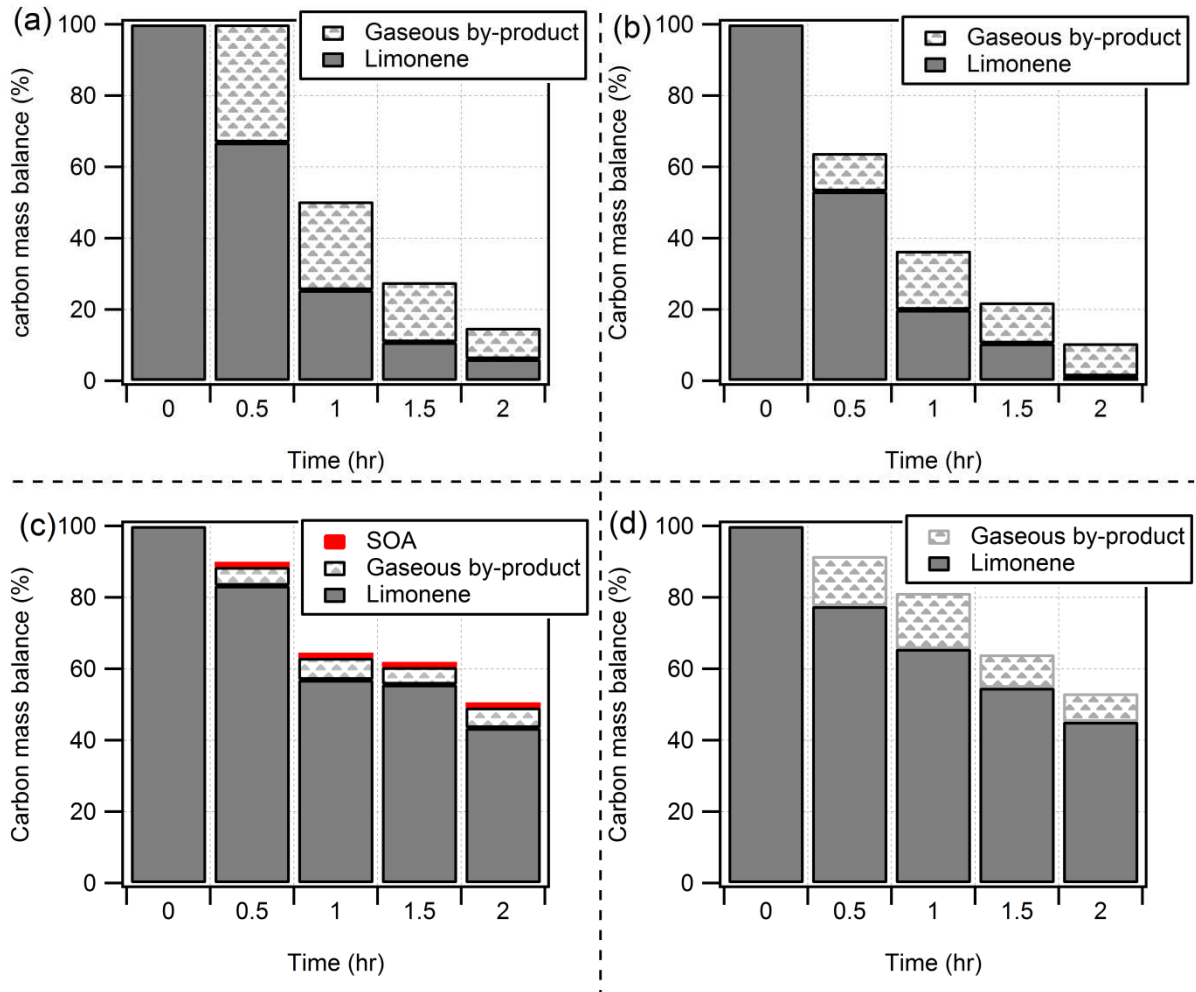


Figure 13 : Respective contribution of limonene, identified gaseous reaction products and particulate matter into the carbon mass balance of VOCs emitted from household products using Device-1 ((a) at startup and (b) after 8h of operation) and Device-2 ((c) at startup and (d) after 8h of operation) ($T^{\circ}C= 22 \pm 1^{\circ}C$; RH=50-60%).

4. Conclusion

A typical and realistic housecleaning action, recognized as a significant source of VOCs indoor, can be performed with a reproducible and controlled protocol in the 40 m³ experimental room IRINA. Typical indoor conditions (23 °C and 50 % RH) lead to the highest VOC emissions from the selected household product. Among monitored emitted VOCs, limonene is from far the most contributing VOC and is evidenced as a relevant tracer to address the fate of VOCs emitted from the selected housecleaning product.

In spite of the fact that selected air treatment devices are characterized by equivalent performances according to current standard in 1 m³ experimental chambers, highly contrasted behaviors have been observed in the large scale experimental room:

- *Primary VOC removal* / The presence of a photocatalytic media in Device-1 combined with UVC irradiation system allows efficient removal of limonene almost 100% accounted to ozone-assisted photocatalysis. In that system adsorption and ozonolysis have been evidenced as minor removal pathways. In contrast, the mix sorptive and photocatalytic media used in Device-2 provides a more than 3 times lower removal of limonene. Adsorption and photocatalysis respectively contribute to 66 and 34 % of the removal process.

- *Side-product formation* / Despite the transient and limited (ca. 40 ppb) pollution peak, both devices lead to carbonyl VOC release in the 40 m³ experimental room; the level of generated side-products can be directly related to the ability of the system to initiate primary VOC oxidation: the higher the removal of primary VOC, the higher the contribution of reaction intermediates to carbon mass balance. The presence of sorptive layer in Device-2 does not show any positive contribution to prevent the release of secondary VOCs. Moreover, the weak oxidative capacity of Device-2 leads to noticeable production of secondary organic aerosols in the experimental room from partial limonene oxidation.
- *10-hour operation* / Treatment performances are not constant with time even on the investigated 10-hour time scale. The limited sorptive capacity and oxidative ability of Device-2 lead to a decrease in the system performances only within 8 hours; in contrast the purely photocatalytic media of Device-1 tend to gain in performances on that time range. The photocatalytic self-cleaning of Device-1 is suggested to interpret that behavior.

Therefore, a reliable evaluation of air treatment processes should: (i) be carried out in a real scale environment on a realistic pollution event; (ii) encompass primary VOC removal as well as secondary VOC generation to define global and relevant performance parameters; (iii) investigate and quantify any possible side-products (secondary VOCs, ozone, particles, etc.) and (iv) address the performances on larger time scales such as several hours or days, combining transient pollution events with continuous pollution background.

Acknowledgment

Authors want to thank the French ADEME (Agence de l'Environnement et de la Maitrise de l'Energie) for its financial support to the project "ETAPE" in the framework of CORTEA research programm and more especially Laurence Galsomies. Mémé Renée is thanked for the ideas provided by her careful cleaning of her bath every Friday.

References

- [1] W.W. Nazaroff, C.J. Weschler, Cleaning products and air fresheners: exposure to primary and secondary air pollutants, *Atmospheric Environment*, 38 (2004) 2841-2865.
- [2] M. Nicolas, J. Nicolle, M. Fernandez, L. Chiappini, C. George, F. Maupetit, Characterization of VOCs and Aldehydes emissions from household products, in: *Indoor Air: Proceedings of the 12th International Conference on Indoor Air Quality and Climate* (2011) 5-10.
- [3] B.C. Singer, H. Destailats, A.T. Hodgson, W.W. Nazaroff, Cleaning products and air fresheners: emissions and resulting concentrations of glycol ethers and terpenoids, *Indoor Air*, 16 (2006) 179-191.
- [4] G. Sarwar, D.A. Olson, R.L. Corsi, C.J. Weschler, Indoor fine particles: the role of terpene emissions from consumer products, *Journal of the Air & Waste Management Association*, 54 (2004) 367-377.
- [5] F. Villanueva, A. Tapia, M. Amo-Salas, A. Notario, B. Cabanas, E. Martínez, Levels and sources of volatile organic compounds including carbonyls in indoor air of homes of Puertollano, the most industrialized city in central Iberian Peninsula. Estimation of health risk, *International Journal of Hygiene and Environmental Health*, 218 (2015) 522-534.
- [6] C. Mandin, M. Trantallidi, A. Cattaneo, N. Canha, V.G. Mihucz, T. Szigeti, R. Mabilia, E. Perreca, A. Spinazzè, S. Fossati, Y. De Kluizenaar, E. Cornelissen, I. Sakellaris, D. Saraga, O. Hänninen, E. De Oliveira Fernandes, G. Ventura, P. Wolkoff, P. Carrer, J. Bartzis, Assessment of indoor air quality in office buildings across Europe – The OFFICAIR study, *Science of The Total Environment*, 579 (2017) 169-178.
- [7] J. Madureira, I. Paciência, J. Rufo, E. Ramos, H. Barros, J.P. Teixeira, E. de Oliveira Fernandes, Indoor air quality in schools and its relationship with children's respiratory symptoms, *Atmospheric Environment*, 118 (2015) 145-156.
- [8] S. Rossignol, C. Rio, A. Ustache, S. Fable, J. Nicolle, A. Meme, B. D'Anna, M. Nicolas, E. Leoz, L. Chiappini, The use of a housecleaning product in an indoor environment leading to oxygenated polar

compounds and SOA formation: Gas and particulate phase chemical characterization, *Atmospheric Environment* 75 (2013) 196-205

[9] M. Nicolas, L. Chiappini, B. D'Anna, Activités domestiques et qualité de l'air intérieur: émissions, réactivité et produits secondaires, ADOQ project, final report, 2013.

[10] L. Morawska, C. He, G. Johnson, H. Guo, E. Uhde, G. Ayoko, Ultrafine Particles in Indoor Air of a School: Possible Role of Secondary Organic Aerosols, *Environmental Science & Technology*, 43 (2009) 9103-9109.

[11] T. Wainman, J. Zhang, C.J. Weschler, P.J. Liroy, Ozone and limonene in indoor air: a source of submicron particle exposure, *Environ Health Perspect*, 108 (2000) 1139-1145.

[12] X. Chen, P.K. Hopke, A chamber study of secondary organic aerosol formation by limonene ozonolysis, *Indoor Air*, 20 (2010) 320-328.

[13] J.Y. Zhang, K.E.H. Hartz, S.N. Pandis, N.M. Donahue, Secondary organic aerosol formation from limonene ozonolysis: Homogeneous and heterogeneous influences as a function of NO_x, *Journal of Physical Chemistry A*, 110 (2006) 11053-11063.

[14] S. Langer, J. Moldanova, K. Arrhenius, E. Ljungström, L. Ekberg, Ultrafine particles produced by ozone/limonene reactions in indoor air under low/closed ventilation conditions, *Atmospheric Environment*, 42 (2008) 4149-4159.

[15] S. Leungsakul, M. Jaoui, R.M. Kamens, Kinetic Mechanism for Predicting Secondary Organic Aerosol Formation from the Reaction of d-Limonene with Ozone, *Environmental Science & Technology*, 39 (2005) 9583-9594.

[16] T. Sun, Y. Wang, C. Zhang, X. Sun, W. Wang, The chemical mechanism of the limonene ozonolysis reaction in the SOA formation: A quantum chemistry and direct dynamic study, *Atmospheric Environment*, 45 (2011) 1725-1731.

[17] A. El Otmani, Oxydation photocatalytique de composés insaturés, terpènes et hétérocycles aromatiques. Effet de l'addition de zéolithes., in, PhD Thesis, Ecole Nationale Supérieure de Chimie de Montpellier, 1993.

- [18] H. Ourrad, F. Thevenet, V. Gaudion, V. Riffault, Limonene photocatalytic oxidation at ppb levels: Assessment of gas phase reaction intermediates and secondary organic aerosol heterogeneous formation, *Applied Catalysis B: Environmental*, 168-169 (2015) 183-194.
- [19] S. Poncet-Vincent, Désodorisation de l'air par photocatalyse au contact de TiO₂: dégradation de l'acide pentanoïque, du limonène et du sulfure d'hydrogène., in, PhD Thesis, Université Claude Bernard Lyon, 1999.
- [20] I. Catanzaro, G. Avellone, G. Marci, M. Saverini, L. Scalici, G. Sciandrello, L. Palmisano, Biological effects and photodegradation by TiO₂ of terpenes present in industrial wastewater, *Journal of Hazardous Materials*, 185 (2011) 591-597.
- [21] M. Saverini, I. Catanzaro, G. Sciandrello, G. Avellone, S. Indelicato, G. Marci, L. Palmisano, Genotoxicity of citrus wastewater in prokaryotic and eukaryotic cells and efficiency of heterogeneous photocatalysis by TiO₂, *Journal of Photochemistry and Photobiology B: Biology*, 108 (2012) 8-15.
- [22] B. Ribot, P. Blondeau, A. Ginestet, F. Squinazi, M. Ott, F. Deblay, Mise en place de protocoles de qualification des appareils d'épuration d'air, rapport final, 2006
- [23] Norme NF EN 16846 Photocatalyse - Mesure de l'efficacité des dispositifs photocatalytiques servant à l'élimination, en mode actif, des COV et des odeurs dans l'air intérieur - Partie 1 : méthode d'essai en enceinte confinée, AFNOR, 2017
- [24] P. Harb, L. Sivachandiran, V. Gaudion, F. Thevenet, N. Locoge, The 40 m³ Innovative experimental Room for INdoor Air studies (IRINA): Development and validations, *Chemical Engineering Journal*, 306 (2016) 568-578.
- [25] O. Debono, F. Thévenet, P. Gravejat, V. Héquet, C. Raillard, L. Le Coq, N. Locoge, Gas phase photocatalytic oxidation of decane at ppb levels: Removal kinetics, reaction intermediates and carbon mass balance, *Journal of Photochemistry and Photobiology A: Chemistry*, 258 (2013) 17-29.
- [26] O. Debono, F. Thevenet, P. Gravejat, V. Hequet, C. Raillard, L. Lecoq, N. Locoge, Toluene photocatalytic oxidation at ppbv levels: Kinetic investigation and carbon balance determination, *Applied Catalysis B: Environmental*, 106 (2011) 600-608.

- [27] Norme XP B 44-013, Méthode d'essai et d'analyse pour la mesure d'efficacité de systèmes photocatalytiques pour l'élimination des composés organiques volatils (COV) / odeurs dans l'air intérieur en recirculation, AFNOR, 2009.
- [28] B. Maquin, C. Jacquioid, D. Lefevre, A. Marchal, J. Patarin, V.P. Valtchev, A.C. Faust, O. Larlus, "Fibre minérale munie d'un revêtement microporeux ou mesoporeux", Patent Fr. 2 827 856 (Saint-Gobain - PL 401055 PCT) 2003
- [29] T. Metts, S. Batterman, Effect of VOC loading on the ozone removal efficiency of activated carbon filters, *Chemosphere*, 62 (2006) 34-44.
- [30] M.A. Sidheswaran, H. Destailats, D.P. Sullivan, S. Cohn, W.J. Fisk, Energy efficient indoor VOC air cleaning with activated carbon fiber (ACF) filters, *Building and Environment*, 47 (2012) 357-367.
- [31] B. Ohtani, S.-W. Zhang, T. Ogita, S. Nishimoto, T. Kagiya, Photoactivation of silver loaded on titanium (IV) oxide for room-temperature decomposition of ozone, *Journal of Photochemistry and Photobiology A: Chemistry*, 71 (1993) 195-198.
- [32] M.A. Smialek, M.-J. Hubin-Franskin, J. Delwiche, D. Duflot, N.J. Mason, S. Vrønning-Hoffmann, G.G.B. de Souza, A.M. Ferreira Rodrigues, F.N. Rodrigues, and P. Limão-Vieira, Limonene: electronic state spectroscopy by high-resolution vacuum ultraviolet photoabsorption, electron scattering, He(I) photoelectron spectroscopy and ab initio calculations", *Physical Chemistry Chemical Physics*, 14 (2012), 2056-2064.
- [33] M.S. Waring, J.A. Siegel, Indoor secondary organic aerosol formation initiated from reactions between ozone and surface-sorbed d-limonene, *Environmental Science & Technology*, 47 (2013) 6341-6348.
- [34] P. Harb, N. Locoge, F. Thevenet, Emissions and treatment of VOCs emitted from wood-based construction materials: Impact on indoor air quality, *Chemical Engineering Journal*, 354 (2018) 641-652.
- [35] H. Kim, S.E. Paulson, Real refractive indices and volatility of secondary organic aerosol generated from photooxidation and ozonolysis of limonene, α -pinene and toluene, *Atmospheric Chemistry and Physics*, 13 (2013) 7711-7723.

- [36] N.L. Ng, J.H. Kroll, M.D. Keywood, R. Bahreini, V. Varutbangkul, R.C. Flagan, J.H. Seinfeld, A. Lee, A.H. Goldstein, Contribution of first-versus second-generation products to secondary organic aerosols formed in the oxidation of biogenic hydrocarbons, *Environmental Science & Technology*, 40 (2006) 2283-2297.
- [37] A.A. Presto, N.M. Donahue, Investigation of alpha-Pinene + Ozone Secondary Organic Aerosol Formation at Low Total Aerosol Mass, *Environmental Science & Technology*, 40 (2006) 3536-3543.
- [38] R.K. Pathak, K. Salo, E.U. Emanuelsson, C. Cai, A. Lutz, A.S.M. Hallquist, M. Hallquist, Influence of Ozone and Radical Chemistry on Limonene Organic Aerosol Production and Thermal Characteristics, *Environmental Science & Technology*, 46 (2012) 11660-11669.
- [39] M. Kalberer, D. Paulsen, M. Sax, M. Steinbacher, J. Dommen, A. Prevot, R. Fisseha, E. Weingartner, V. Frankevich, R. Zenobi, Identification of polymers as major components of atmospheric organic aerosols, *Science*, 303 (2004) 1659-1662.
- [40] Y. Pang, B. Turpin, L. Gundel, On the importance of organic oxygen for understanding organic aerosol particles, *Aerosol Science and Technology*, 40 (2006) 128-133.
- [41] A.P. Bateman, S.A. Nizkorodov, J. Laskin, A. Laskin, Time-resolved molecular characterization of limonene/ozone aerosol using high-resolution electrospray ionization mass spectrometry, *Physical Chemistry Chemical Physics*, 11 (2009) 7931-7942.

